

Is Energy Resolution Still an Important Specification in EDS?

Keith Thompson

Thermo Fisher Scientific, 5225 Verona Rd., Madison, WI 53711

keith.thompson@thermofisher.com

Introduction

Energy Dispersive Spectroscopy (EDS) X-ray detectors have undergone a wave of technology enhancements since the first silicon drift-based EDS detector (SDD) was commercially introduced roughly 15 years ago. The first such EDS systems featured an active area of 5 mm², an energy resolution between 160 eV–200 eV, and a maximum collection rate approaching only 100,000 input counts/second.

Today, commercial SDD-based EDS detectors feature active areas up to 150 mm² per device with multiple detectors commonly working in tandem. Collection rates of 1 million input counts/second are an expected standard. Spectral energy resolution down to 121 eV is now available.

Although energy resolution as measured and reported today is an important metric, it oversimplifies detector performance. When targeting actual end-user applications, a more in-depth evaluation and a much broader specification is required. This article addresses these issues.

Energy Resolution and the Entire Energy Spectrum

Now that energy resolution is approaching its theoretical limit [1], how important are further advances in energy resolution? And what other factors or techniques now play a more dominant role?

An EDS spectrum of a BN sample, whose surface was conveniently contaminated with C and O, is shown in Figure 1. An EDS spectrum of Be, whose surface was also contaminated with C and O is shown in Figure 2. These spectra show very clean and well-separated Be or B peaks, as well as N, C, and

O peaks. The energy resolution for the EDS detector used to collect these data, as measured at Mn K α , is 122 eV. The energy resolution of the C peak in both spectrums is 39 eV.

While impressive, the advanced SDD represents only half of the improvement required to produce the spectra described above. Attenuation of low-energy X rays presents serious challenges to low-energy X-ray analysis. These X rays are attenuated by many sources. First, the window used to isolate the SDD crystal from the microscope vacuum (or ambient while vented) absorbs low-energy X rays. Traditional Be windows prevented transmission of X rays lower than the Na K α line (~1 keV) and should therefore be eliminated as an option. Second, any inert gas between the SDD crystal and the window will absorb low-energy X rays. In many designs inert N₂ gas is intentionally used to back-fill the volume between the SDD crystal and the light-element window. The degradation of low-energy sensitivity by inert N₂ gas can be simulated by applying the X-ray absorption curves for N₂ gas across the distance the X rays must travel through the N₂ gas. These simulated spectra are plotted in Figures 1 and 2. When compared against a detector whose volume is fully evacuated, as opposed to back-filled with N₂, the difference in low-energy sensitivity is stark. Finally, the sample itself absorbs low-energy X rays if they are generated deeper than the average escape depth for that energy. Lithium, for example, has an escape depth of only a few tens of nm. As a result, even a small amount of surface contamination presents extreme challenges to detecting Li with any EDS detector.

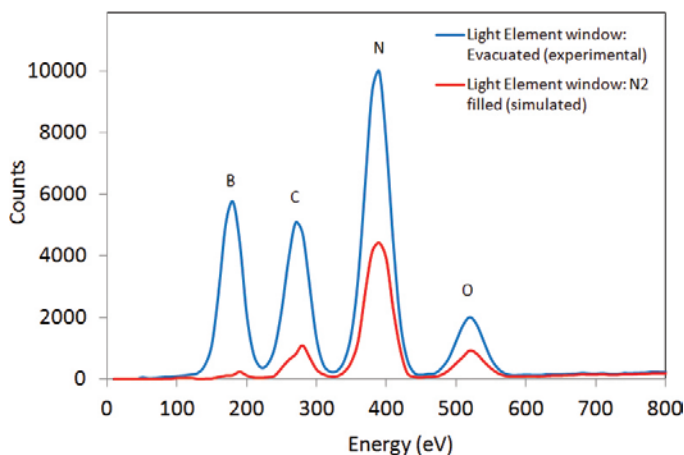


Figure 1: EDS spectrum of BN with C and O surface contamination as obtained with a fully evacuated EDS X-ray detector employing an ultra-thin, polymer window (blue), and the simulated spectrum if the detector module were back-filled with inert N₂ (red).

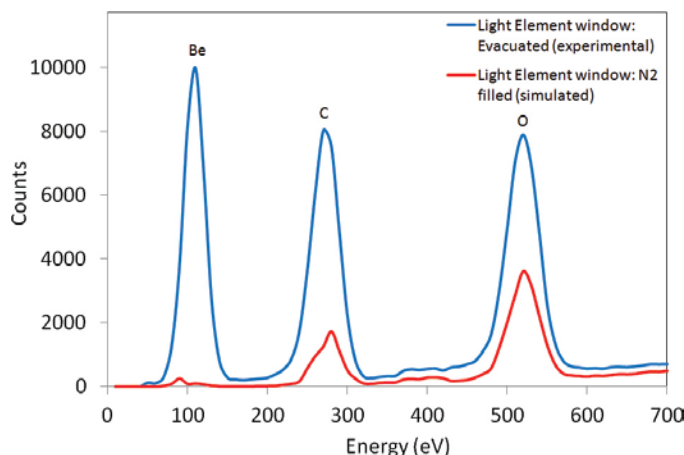
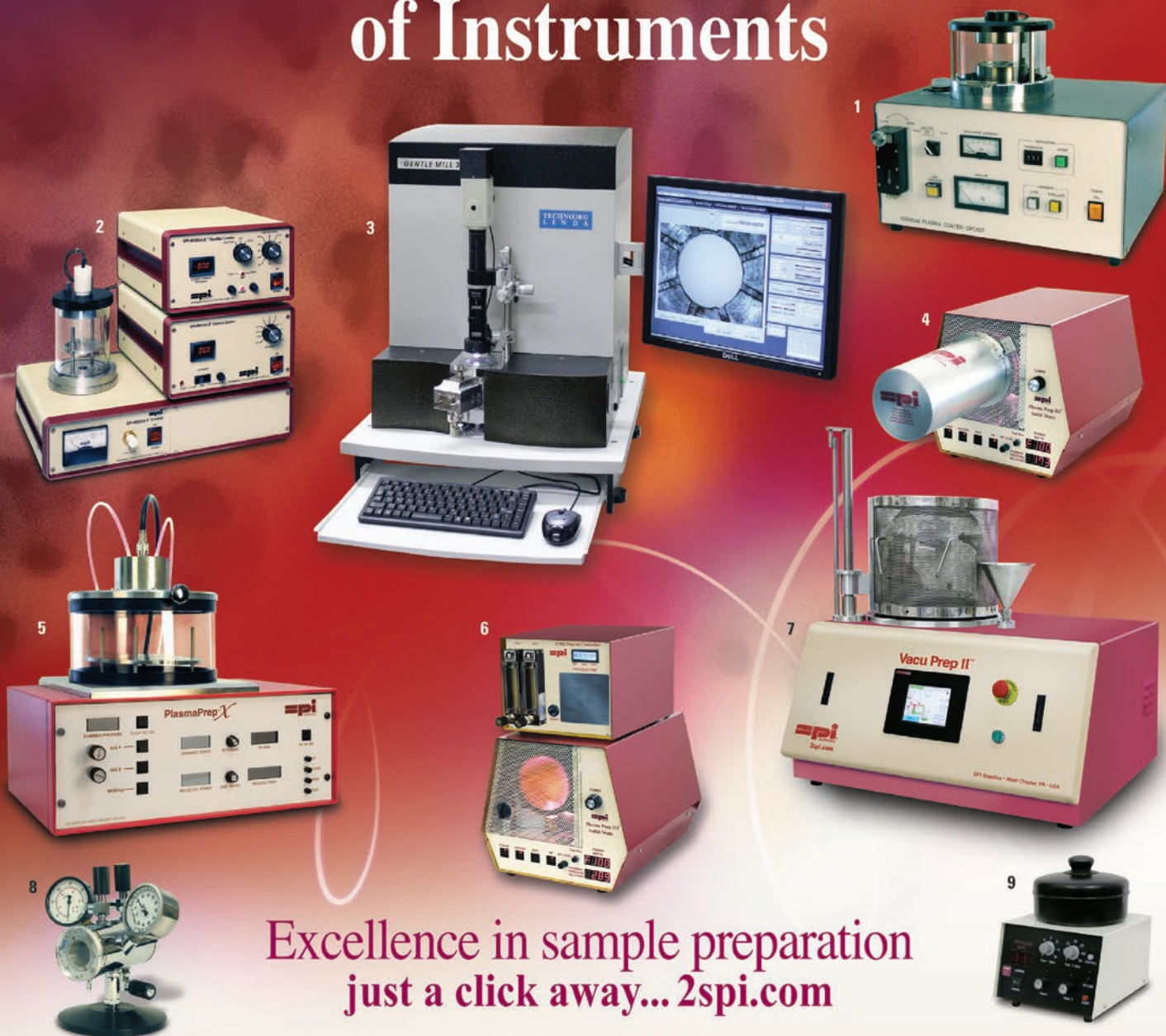


Figure 2: EDS spectrum of Be with C and O surface contamination as obtained with a fully evacuated EDS X-ray detector employing an ultra-thin, polymer window (blue), and the simulated spectrum if the detector module were back-filled with inert N₂ (red).

The SPI Supplies Family of Instruments



Excellence in sample preparation
just a click away... 2spi.com

Your results will never be better than your sample preparation. See how SPI Supplies can help you deliver the highest quality results for all your SEM/EDS, TEM and FESEM applications.

1. Osmium Plasma Coaters for FESEM Applications
2. SPI-MODULE™ Sputter/Carbon Coater Module
3. Gentle Mill™ Ion Milling System
4. Plasma Prep™ III Solid State Plasma Cleaner for cleaning TEM holders

5. Plasma Prep™ X Parallel Plate Plasma Etcher
6. Plasma Prep™ III Plasma Etcher with PPIII Process Controller
7. Vacu Prep™ II Turbo Pump Evaporation System
8. SPI-DRY™ Critical Point Dryer
9. Precision Spin Coater Spin coater



SPI Supplies Division of STRUCTURE PROBE, Inc.

P.O. Box 656 • West Chester, PA 19381-0656 USA
Phone: 1-610-436-5400 • 1-800-2424-SPI (USA and Canada) • Fax: 1-610-436-5755 • 2spi.com • E-mail: sales@2spi.com



As a result, low-energy detection is best attained by first using either an ultra-thin, polymer window (< 300 nm) or by eliminating the window altogether. Nitrogen gas should not be used to backfill the volume between the thin window and the SDD module if detection below 300 eV is desired. A fully evacuated detector module (or a completely windowless detector) should be employed. Finally, because of X-ray absorption within the sample itself, one should rely primarily on analysis of the top 10–50 nm of the sample. This forces no requirement on the SDD but does imply: (1) extreme care in preparing and in preserving the sample surface and (2) operating the SEM at a shallow penetration depth (< 5 kV) to avoid diluting the low-energy analysis of the surface region with the high-energy X rays generated from the overall bulk of the sample.

Energy Resolution and Count Rates

Although an energy resolution of 121 eV that pushes the Bremsstrahlung limit is impressive, it is rarely witnessed during normal operation. This energy resolution is typically specified at an input count rate of < 5000 counts per second. At these low rates, a peaking time of > 6.4 microseconds can be employed. Shorter peaking times, which are required for high count rate acquisition, result in a greater statistical uncertainty in the energy of the collected X ray and therefore a lower energy resolution [2, 3]. Figure 3 shows the optimal peaking times and resulting impact on energy resolution required to acquire spectra at a maximum dead time of 50%. The energy resolution in this graph changes from 125 eV at 6.4 microseconds up to 175 eV at 0.2 microseconds.

Most mapping applications with an SDD occur at an *output* count rate of a few hundred thousand counts per second. At a 50% dead time, the ratio of input and output count rates is 2. This ratio will be higher at higher dead times. Mapping at 200,000 input counts/second (100,000 output counts/second), however, results in a resolution degradation of roughly 8 eV at a 1-microsecond time constant. Forced operation at a long time constant prevents this degradation but also results in very slow acquisition rates (few thousand output counts per second) as the very high dead time limits overall throughput. This situation is unsuitable for mapping. A system that allows multiple peaking times, as opposed to only 2 or 3 peaking times, provides a de facto advantage in energy resolution because the longest possible peaking time can be automatically selected for any given input count rate.

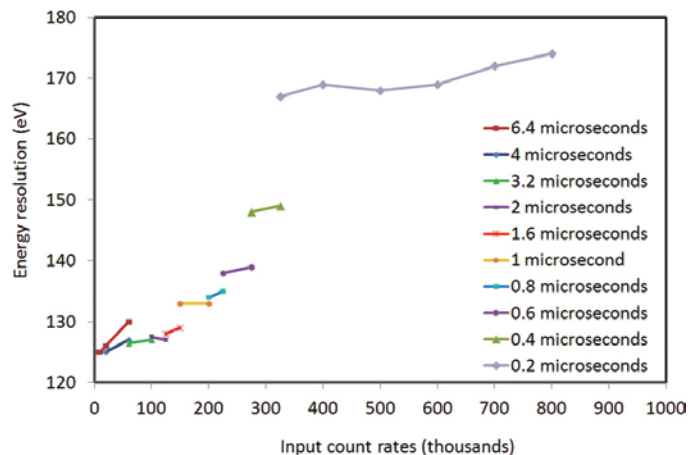


Figure 3: Energy resolution as a function of input count rates at 50% dead time (output count rate is approximately half of input count rate).

The end result is that certain designs may demonstrate an energy resolution of 121 eV at < 5000 input counts per second but only achieve an energy resolution of 140–150 eV in mapping mode when output counts exceed 100,000 per second. Thus, a broader specification for energy resolution, which includes both high- and low-throughput requirements, would be more useful to the end user.

Energy Resolution and Post-Processing Algorithms

Another consideration related to enhanced energy resolution involves the actual spacing of the X-ray lines generated by the elements within the sample itself. Although the spectra in Figures 1 and 2 elegantly present the value of an improved EDS detector, the elements Be, B, C, N, and O all result in single X-ray lines within the spectrum that are separated by 150 eV–250 eV.

By comparison, consider the EDS spectrum in Figure 4. The sample analyzed was galena, which is composed pri-

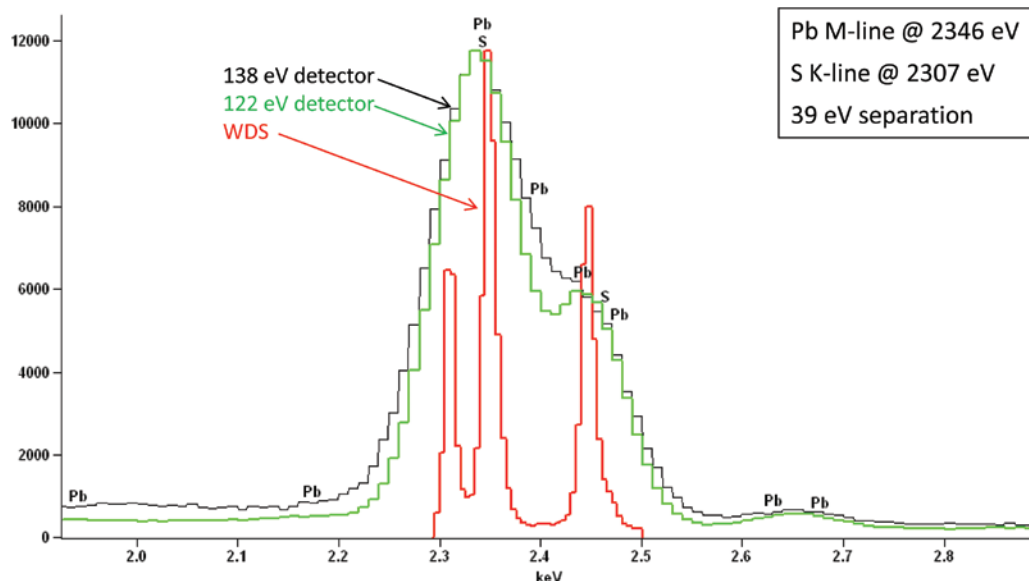


Figure 4: Energy-dispersive X-ray spectrum of galena (primarily Pb and S) for: (a) an SDD at 138 eV (circa 2002), (b) an SDD at 122 eV (circa 2012), and (c) a Magnaray™ WDS spectrometer. The principal lines resolved by the WDS are the S K α at 2.31 keV, the Pb M α at 2.34 keV, and the combined peak of Pb M β at 2.44 keV convolved with S K β at 2.46 keV.

marily of Pb and S with the formula PbS. The S K-line (2.307 keV) and the principal Pb M-line (2.346 keV) are separated by only 39 eV. Furthermore, there are multiple Pb M-lines. The sample was analyzed with two different EDS detectors: the first with an energy resolution of 138 eV, and the second with an energy resolution of 122 eV. Finally the sample was also analyzed with a Thermo ScientificTM MagnaRayTM wavelength dispersive spectrometer (WDS). The 122 eV detector spectrum exhibits improvement relative to that of the 138 eV detector. Despite the 16 eV improvement in energy resolution, however, the Pb and S peaks still overlap significantly. No clear distinction between the elemental X-ray lines exists. An energy resolution well below 40 eV would be needed to achieve serious separation of the peaks. Only a WDS, which has superior energy resolution, accurately resolves the S K-line and the Pb M-lines into separate peaks.

It is clear that the continued presence of closely spaced X-ray lines will always result in overlapping peaks when

even the best EDS detector is employed. This prevents direct observation of unidentified specimen elements. This creates not only a challenge to qualitative and quantitative analysis but also to effective element mapping. Fortunately, a solution can be found by the appropriate application of post-processing algorithms.

Figure 5a shows the element maps of the galena sample plotted with “gross” X-ray counts. In other words, with X-ray counts that were not corrected after acquisition. Also shown, for reference, is the WDS element map for Pb and for F. The elements identified as present by the EDS spectrum are Pb, O, F, S, Ca, Mn, Cu, As, and Sb. Three regions are evident within the map: (Phase 1) a phase at middle-left and middle-right comprised mainly of Ca and F; (Phase 2) a phase at center composed mainly of Cu and S; and (Phase 3) a matrix material of Pb and S. The mapped backgrounds are quite high for several elements, including O, Mn, Cu, and As. This indicates either a consistent, low-level distribution of these elements

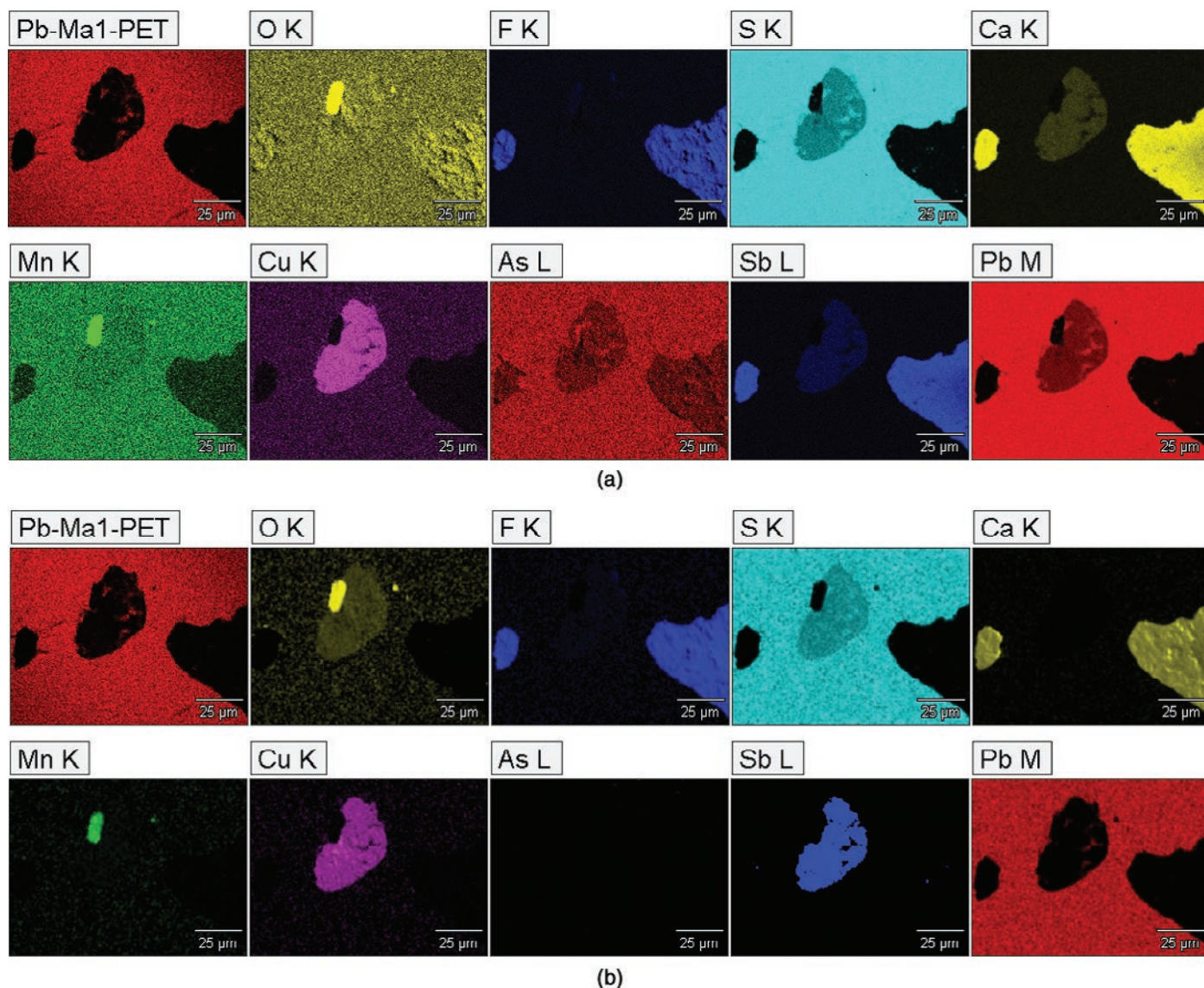


Figure 5: (a) X-ray element maps of a galena (PbS) sample exhibiting “gross” or uncorrected X-ray counts. (b) The same X-ray element maps of (a) but with corrections for peak deconvolution and background subtraction.

throughout the sample or consistent mis-identification of the elements due to peak overlaps within the spectrum. There are also “ghost-like” regions of Ca and Sb in Phase 2. One might dismiss the “ghost-like” Ca and Sb distribution as artifacts. Without further evidence, however, this is a dangerous assumption. In addition, the EDS map for Pb does not match the WDS map for the Pb M-alpha line; another indication that peak overlaps have created errors within the EDS mapping results.

Figure 5b shows the same element maps, using the exact same raw data. This time, however, a peak deconvolution, a matrix correction, and a background subtraction algorithm were all applied to the collected spectra in each pixel, colloquially referred to as “quantitative elemental mapping” or “quant maps.” The impact of these maps is immediately evident when the element maps in Figures 5a and 5b are compared.

First, the overall image noise around the concentrations of several elements—in particular O, Mn, and Cu—falls to zero or near zero except in the actual phase where it is found to exist. Second, the As counts go to zero everywhere. It is now evident that the As, originally identified by the As K-line at 10.532 keV, is indeed an overlap with the Pb L-lines at 10.549 eV. Third, the EDS identification of Pb in the central Cu-S region (that is, Phase 2) is eliminated, bringing the wt% map of Pb in direct alignment with the WDS map of Pb. Fourth, S still exists in both the central region and the matrix region around it. This helps to clearly identify a Cu and S containing region for Phase 2 surrounded by a Pb-S, or galena, matrix material in Phase 3. Fifth, regarding the Ca and Sb “ghost-like” distributions in Phase 2, the Ca distribution found in the Cu-S region has disappeared completely. The Ca and F are now uniquely isolated to Phase 1, identifying this region as fluorite (CaF_2). And sixth, the quant map clarifies that the Sb, although not present in Phase 1, is indeed present in the Cu-S Phase 2 region. This rejects any hypothesis that the Sb located in this region is an artifact. The presence of Sb in Phase 2 changes the phase type from copper sulfide to chalcostibite (CuSbS_2).

This mapping exercise identified 6 major flaws in a single sample when analyzed using basic mapping techniques and a state-of-the-art, 122 eV resolution EDS detector. Although EDS detectors have advanced significantly in terms of energy resolution over the last decade, it is evident that until energy resolution reaches the level of WDS, efficient post-processing algorithms will remain significantly more important for improving element mapping than any further improvements in energy resolution.

Summary

EDS detectors have advanced significantly over the last 15 years. The consistent improvements in energy resolution (from > 160 eV to < 130 eV) have played an important role in developing the current state of EDS technology. However, energy resolution represents only one of many factors in obtaining world-class EDS data. Thin-window or windowless technologies and the elimination of any inert gas between the

thin window and the SDD crystal are critical to low-energy detection. During mapping applications, fast electronics and low-capacitance SDDs are critical to minimizing the degradation in energy resolution that necessarily occurs at output counts rates of a few hundred thousand per second. Finally, although an extreme EDS energy resolution generates aesthetically pleasing spectra, powerful post-processing algorithms provide the most powerful lever (short of full WDS element mapping) for producing high-quality, accurate EDS elemental maps.

References

- [1] J Goldstien, DE Newbury, DC Joy, CE Lyman, P Echlin, E Lifshin, L Sawyer, and JR Michael, *Scanning Electron Microscopy and X-ray Microanalysis*, Springer, New York, 2003, pp. 311–12.
- [2] L Strueder, N Meidinger, D Stotter, J Kemmer, P Lechner, P Leutenegger, H Soltau, F Eggert, M Rohde, and T Schulein, “High Resolution X-Ray Spectroscopy Close to Room Temperature,” *microanalyst.net*, published online July 1998, http://mikroanalytik.de/Download/sdd_publ.pdf.
- [3] Amptek, Inc., “Amptek Silicon Drift Diode (SDD) at High Count Rates: AN-SDD-001 Rev B0,” <http://www.amptek.com/pdf/ansdd1.pdf>.

MT

tousimis
WINNER OF 2012
MICROSCOPY TODAY
INNOVATION AWARD

tousimis® touchscreen 931
• CPD Recipe Capable Automation
• Multi-Application Critical Point Dryer

www.tousimis.com © 2013 tousimis®

The single source for all your **microscopy supplies** and **specimen preparation equipment.**



- PELCO BioWave® Pro Tissue Processor

- PELCO *easiGlow*™ Glow Discharge Unit

- SEM Sample Holders and Mounts

- EM Sample Coating Systems

- Calibration Standards

- PELCO® Quality Tweezers

- Grinder / Polishers

- SEM Supplies

- TEM Support Films

- AFM Supplies

- Conductive Adhesives

- FIB Supplies



COMPLETE LINE OF CRESSINGTON EM SAMPLE COATERS AVAILABLE

 **TED PELLA, INC.**
Microscopy Products for Science and Industry

www.tedpella.com sales@tedpella.com 800.237.3526